Available online at www.sciencedirect.com

SCIENCE DIRECT®

Chemical Physics 326 (2006) 577–582

Chemical Physics

www.elsevier.com/locate/chemphys

Synthesis of terahertz electromagnetic wave pulses using amplitude-and-phase masks

Ryuzi Yano [a,*,1], Hideki Gotoh [a], Yoshiro Hirayama [a], Toshiaki Hattori [b], Sen Miyashita [c]

[a] *NTT Basic Research Laboratories, NTT Corporation, 3-1, Morinosato-Wakamiya, Atsugi-shi, Kanagawa 243-0198, Japan*

[b] *Institute of Applied Physics, University of Tsukuba, Tsukuba 305-8573, Japan*

[c] *NTT Advanced Technology, 3-1, Morinosato-Wakamiya, Atsugi-shi, Kanagawa 243-0198, Japan*

Received 15 August 2005; received in revised form 20 February 2006; accepted 16 March 2006
Available online 22 March 2006

Abstract

In the conventional terahertz (THz) electromagnetic emission and detection scheme using a semiconductor as a THz wave emitter and a photoconductive antenna as a THz wave receiver, we generated THz electromagnetic waves having various temporal waveforms by inserting simple plastic plates between off-axis parabolic mirrors. We simulated the observed waveforms using a simple model, where the THz field is expressed by the summation of fields passing through each sub-section of the whole cross-section of the collimated THz beam. The results show a new simple method to shape THz pulses with complicated temporal waveforms.

JEL classification: 42.65.Re; 42.79.−*e*

Keywords: Terahertz electromagnetic waves; Pulse shaping

1. Introduction

Recently, there has been a growing interest in temporally arbitrary pulse generation or pulse shaping in the terahertz (THz) frequency or millimeter wavelength regions [1–8]. Such THz or millimeter wave pulses can be applied for the investigation of ultrafast dynamics and for the coherent control of the dynamics in materials [9–12]. Arbitrary shaped electric fields can be applied to atoms or molecules to change their transition frequencies temporally (this technique is the generalization of AC Stark switching [13]), and thereby assist the control of the reaction or the dynamics of molecules or atoms. Also, transient alignment of the dipoles of atoms or molecules will become possible by using arbitrarily shaped THz fields.

Generally, temporally shaped THz pulses are generated by exciting a THz emitter using shaped laser pulses [1–4,20] or by modifying or spectrally filtering THz waves themselves [5–8]. In the first method, the excitation laser pulses are often shaped using a liquid crystal spatial mask in a four-lens configuration or using interference between two time-delayed chirped laser pulses. In the second method, gratings for millimeter waves, prism pairs, and apertures have been used to generate shaped THz pulses. However, by using these methods, mainly frequency-tunable, frequency-chirped, or low-frequency-cut-off THz pulses have been produced. So far, a few reports have been shown to generate more complex THz waves [20]. We note here that use of all the frequency components of the THz wave is required for generation of temporally arbitrary THz waves.

In this paper, we describe a simple method for generating temporally complicated THz pulses. In the method, THz waves are directly modified using amplitude-and-phase masks whose size is much larger than the typical wavelength of THz waves. This method is useful especially when THz

* Corresponding author. Tel.: +81 143 46 5613; fax: +81 143 46 5601.
E-mail address: ryie1@mmm.muroran-it.ac.jp (R. Yano).

[1] Present address: Muroran Institute of Technology, 27-1, Mizumoto-cho, Muroran, Hokkaido 050-8585, Japan.

0301-0104/$ - see front matter © 2006 Elsevier B.V. All rights reserved.
doi:10.1016/j.chemphys.2006.03.021

waves are generated without the use of laser pulses, and complex THz waveforms can be obtained by directly shaping THz waves. We generated various complex temporal waveforms of THz waves by inserting a mask such as a plastic plate, between a pair of off-axis parabolic mirrors, which are often used to collimate THz waves generated from an emitter.

In our setup, the THz source can be regarded roughly as a point source, and we ignored the effect of diffraction after collimating the source. We show experimentally that the observed THz waveforms can be synthesized by the summation of THz fields that have passed through sub-sections of the THz beam. Simulation based on a simple model well reproduced the experimentally obtained THz waveforms. We also show the possibility that an aperture can be used to reduce the pulse width of the THz wave. Generation of temporally complex THz waveforms based on our model is simple. Therefore, the calculation of the properties of masks is not complicated.

2. Experiment

The experimental setup is shown in Fig. 1(a). The output (center wavelength of about 790 nm, pulse width of about 300 fs, repetition rate of 82.2 MHz) of a mode-locked Ti:Al_2O_3 laser was divided by a beam splitter into pump and gate pulses. The pump pulses were focused by a lens to a spot size of about 100 μm (e^{-2} spot size) and excited an InAs sample to generate THz electromagnetic waves.

The THz emitter was a 0.5-μm-thick wafer of undoped InAs. The estimated average photogenerated carrier density was about 1×10^{17} cm^{-3} for 140 mW average excitation power, assuming the absorption coefficient α at 790 nm to be 10^4 cm^{-1}. The gate pulses were focused by an objective lens to a diameter of about 6 μm and excited a photoconductive (PC-) antenna fabricated on low-temperature grown (LT-) GaAs. The carrier lifetime of the LT-GaAs measured by pump–probe spectroscopy [14] was about 0.5 ps. The average power of the gate pulse was 2 mW.

The THz electromagnetic waves emitted from the surface of the InAs were collected and guided to the PC-antenna using a pair of off-axis parabolic mirrors, which had a reflected effective focal length of 100 mm and a diameter of 50 mm. The gate pulses generated photo-excited carriers in the PC-antenna. Electric current that flows in the PC-antenna should be proportional to the instantaneous THz field amplitude. An optical chopper was used to modulate the intensity of the pump pulses at a frequency of 1.3 kHz. The current in the PC-antenna was amplified and fed to a lock-in amplifier. To obtain the temporal profile of the THz electromagnetic waves, the output of the lock-in amplifier was measured while the delay between the pump and gate pulses was changed. In order to modify the THz waveforms, we inserted a mask or an aperture between the parabolic mirrors.

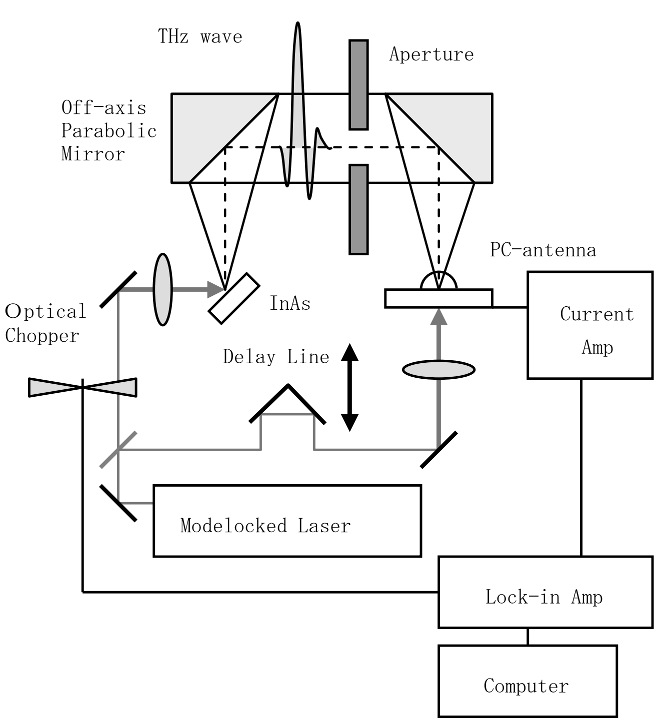

Fig. 1. Experimental setup for THz pulse shaping.

3. Experimental results and discussions

We first show examples of complex temporal THz waveforms obtained using simple masks. We next characterize the THz wave properties to build a theoretical model for understanding the synthesis of the observed waveforms. We show the results of the measurement of aperture-size dependence of the temporal profiles of the THz wave and discuss the possibility of pulse-width narrowing of THz waves. Then, we describe the principle of the waveform synthesis in our experimental conditions and show results of simulations of the observed waveforms based on the idea.

3.1. Pulse shaping using simple masks

Solid curves in Figs. 2(a)–(d) show examples of THz waveforms obtained by inserting simple masks between the off-axis parabolic mirrors. Fig. 2(a) shows a triangular wave with increasing amplitude, which was obtained by inserting a 22-mm-wide, 100-mm-long, 0.40-mm-thick plastic plate in the center of the cross-section of the THz wave. The plate in this case was the stand for a table-top calendar. The waveform shown in Fig. 2(b) consists of a half-cycle and monocycle THz pulses, which were obtained by inserting the same plastic plate 7 mm above the center of the cross-section. As shown in Fig. 2(c), an oscillation with decreasing amplitude was obtained by masking half area of the cross-section of the THz beam with the same plastic plate. A letter-N-shaped waveform (Fig. 2(d)), was obtained by inserting a 22-mm-wide, 300-mm-long, 2.0-mm-thick plastic ruler in the center of the cross-section of

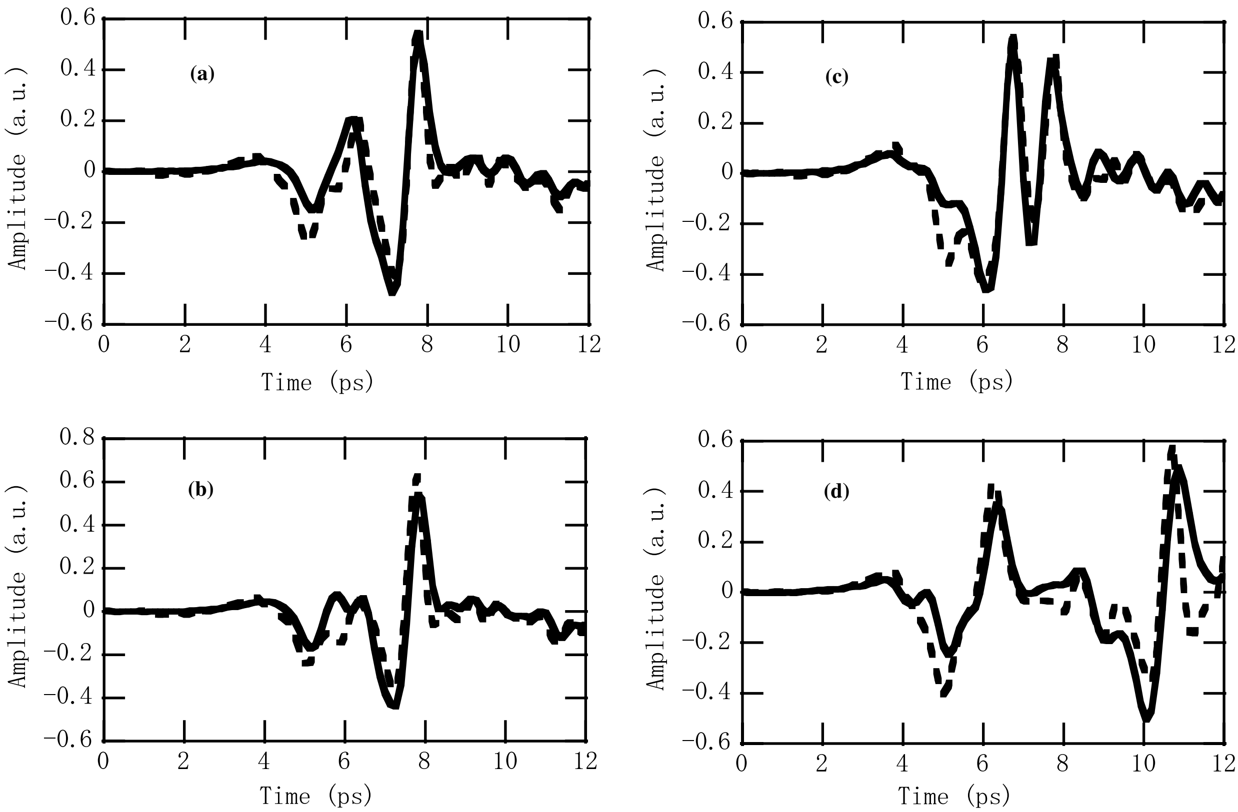

Fig. 2. Temporal profiles of THz waves obtained using simple masks. Solid curves in (a)–(c) were obtained using a plastic plate originally used as a calendar stand. The solid curve in (d) was obtained using a plastic ruler. The dashed curve in each figure is the simulation result based on Eq. (2).

the THz wave. These THz waveforms show that various complex THz waveforms can be generated using simple masks.

3.2. THz wave properties

We observed change in the THz waveform induced by insertion of a metal aperture between the off-axis parabolic mirrors. Fig. 3 shows the temporal profiles of the THz wave obtained (a) without an aperture (corresponding to aperture diameter of 50 mm), using an aperture diameter of (b) 30, (c) 20, and (d) 10 mm. The observed temporal profile of the THz wave changed largely as the aperture size changed.

Since the divergence angle of the THz wave is proportional to the THz wavelength, we expected that, if we used only the center section of the THz beam, we would obtain a shorter THz-pulse duration. Looking Fig. 3 again, we notice that the THz pulse width became smaller for smaller aperture size (The temporal component of the THz wave from 4 to 6 ps region was deleted, and the overall pulse width was shortened). The difference of the relative phase of the frequency components of the THz spectrum between inner and outer cross-sections divided by a 10-cm diameter aperture reduced the THz pulse width.

The Fourier amplitudes of the temporal profiles of Fig. 3(a) (without aperture) and Fig. 3(d) (10-mm aperture diameter) are shown in Fig. 4 by dashed and solid curves, respectively. In obtaining the THz spectra, we normalized the temporal profiles of the THz waves and performed Fourier transformation. We clearly see that, at the 10-mm aperture diameter, the amplitude of low-frequency components (<0.5 THz) actually decreased compared with the THz spectrum without an aperture [15,21]. This result shows that pulse-width narrowing is possible using an aperture for eliminating the outer side of the cross-section of the THz beam.

Since the size of the THz wave emission area on the InAs wafer surface was about 100 μm, it was not a perfect point source. We collimated such THz waves by an off-axis mirror. Therefore, it was not a perfect collimation of the THz wave in principle. We measured the aperture-position dependence of the peak-to-peak amplitude of the THz wave at several points between the off-axis parabolic mirrors. The observed peak-to-peak amplitude of the THz wave obtained using aperture diameters of 10 and 20 mm did not depend on the aperture position largely. This shows that the collimation of the THz beam in the present setup was sufficiently good, and our THz beam can be regarded roughly as being emitted from a point source. The distance between the mask and the receiver (PC-antenna) was about 190 mm in the measurements described below.

The effective focal length L of the off-axis parabolic mirror was about 100 mm, and the typical size a of masks was large compared with the typical THz wavelength λ. The estimated spot size D of the THz waves at the receiver's

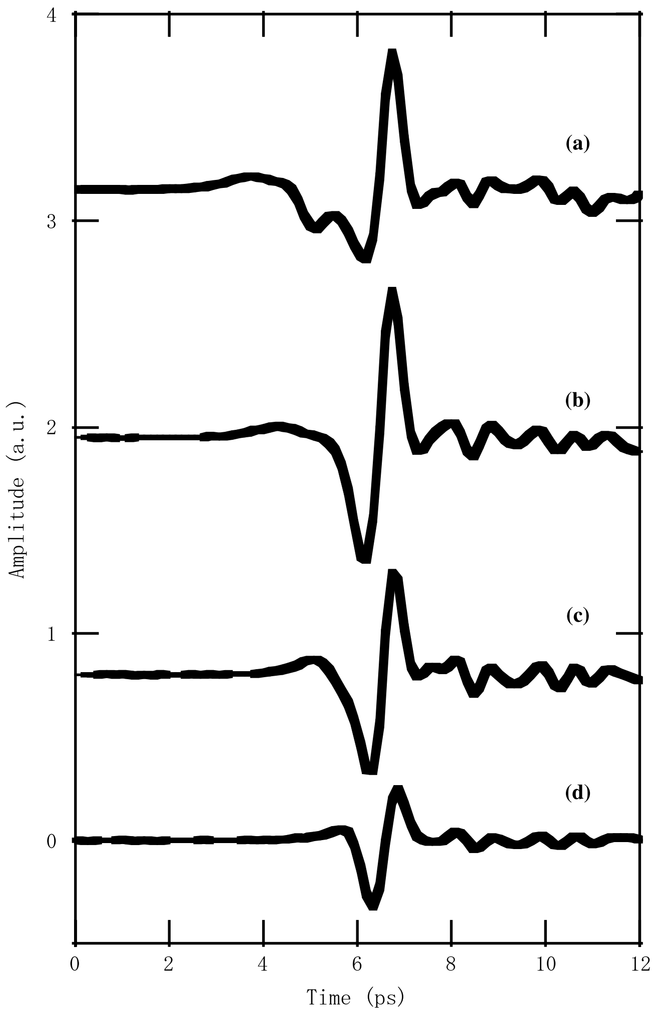

Fig. 3. Temporal profiles of the THz waves obtained (a) without an aperture, and using (b) a 30-mm-diameter aperture, (c) a 20-mm-diameter aperture, and (d) a 10-mm-diameter aperture. The zero-base lines of the four figures were shifted to avoid confusion.

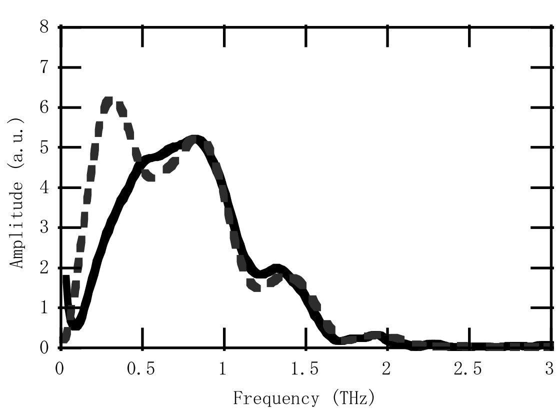

Fig. 4. Fourier amplitude of the THz waves shown in Fig. 3(a) (dashed curve, without aperture) and Fig. 3(d) (solid curve, 10-mm aperture).

position without a Si lens was $D \sim L(\lambda/a) \sim 1$ mm [16]. Therefore, we expected that the effect of diffraction by the masks on the temporal profiles of the THz waves would not be large.

To verify this idea in the THz wavelength region, we divided the cross-section of the THz wave into two subsections S_{win} and S_{wout}, which were divided by a 25-mm diameter circle centered at the center of the THz wave cross-section (as shown in the left side of Fig. 5) and measured the temporal profiles of the THz waves that have passed through one of the two subsections. The THz waves obtained were compared with those obtained using the whole cross-section of the beam. Aluminum foil was used to mask the unused section of the THz beam.

Fig. 6(a) shows the THz waveform obtained using only the outer section (solid curve, corresponding to the sub-cross-section S_{wout} in Fig. 5) and only the inner section (dashed curve, corresponding to the sub-cross-section S_{win} in Fig. 5). Fig. 6(b) shows the THz waveform obtained without any masks (solid curve) and that obtained by summation of the two THz waveforms shown in Fig. 6(a) (dashed curve). The agreement between the two THz waves shown in Fig. 6(b) is quite good. This result shows that the effect of the diffraction by the edges of masks can be neglected in our experimental conditions and that the THz waves detected by the receiver can be given by the summation of the THz wave that has passed through each sub-cross-section.

3.3. Simulation of THz waves

Based on the experimental results shown above, we constructed a simple model of the THz wave shaping. The THz wave $E_{\text{mask}}(t)$, which is detected by a receiver after it is modified by a mask, can be obtained by simply summing up all the contributions of the sub-sections of the THz, and is given by

$$E_{\text{mask}}(t) = \int\int A(\omega, r)\exp[-\mathrm{i}\varphi(\omega, r)]E_{\text{in}}(\omega, r) \times \exp[-\mathrm{i}\phi(\omega, r)]\exp(-\mathrm{i}\omega t)\,\mathrm{d}r\,\mathrm{d}\omega \tag{1}$$

Here, $E_{\text{in}}(\omega, \mathbf{r})\exp[-\mathrm{i}\phi(\omega, \mathbf{r})]$ is the complex amplitude of the incident THz waves at frequency ω and position $\mathbf{r}$ within the cross-section of the THz wave, $A(\omega, \mathbf{r})\exp[-\mathrm{i}\varphi(\omega, \mathbf{r})]$ represents the properties of the mask at frequency ω and position $\mathbf{r}$ that changes the amplitude from unity to $A(\omega, \mathbf{r})$ (amplitude mask), the phase from zero to $\varphi(\omega, \mathbf{r})$ (refractive-index or phase mask, which can cause a time delay). Therefore, our method does not use only a limited wavelength region. It should also be noted that this method is concerned with the modification of the THz waves observed at the receiver's position, and that the contribution of each sub-cross-section to the observed THz waveform is not necessarily the same. We usually collimate pulses to a certain small spot and probe or excite materials. Therefore, for most material studies we do not necessarily need a THz pulse with a large spatially uniform cross-section.

Temporally arbitrary THz waves can be obtained using suitable masks that satisfy Eq. (1) if we know all the spatial

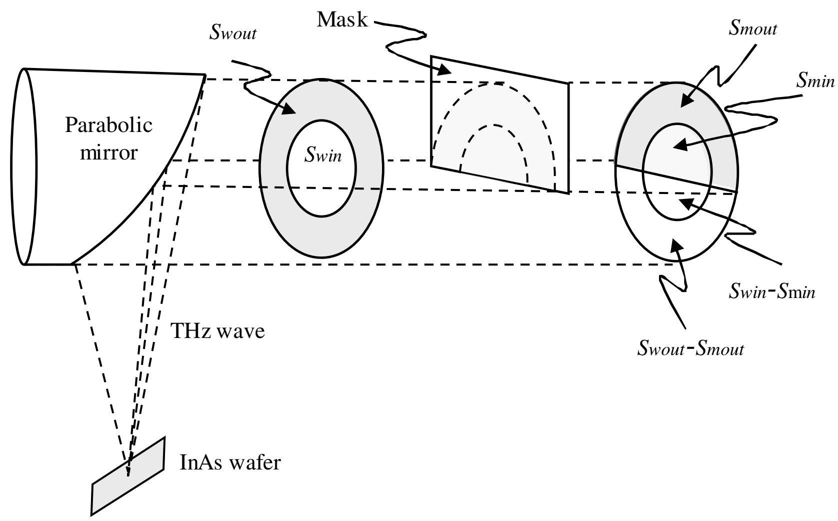

Fig. 5. Illustration of cross-sections of a THz wave. S_{win} and S_{wout} are areas of inner and outer cross-sections. S_{min} and S_{mout} are areas of the inner and outer cross-sections covered by a mask. The diameter of S_{wout} was limited by the diameter (50 mm) of the off-axis mirror.

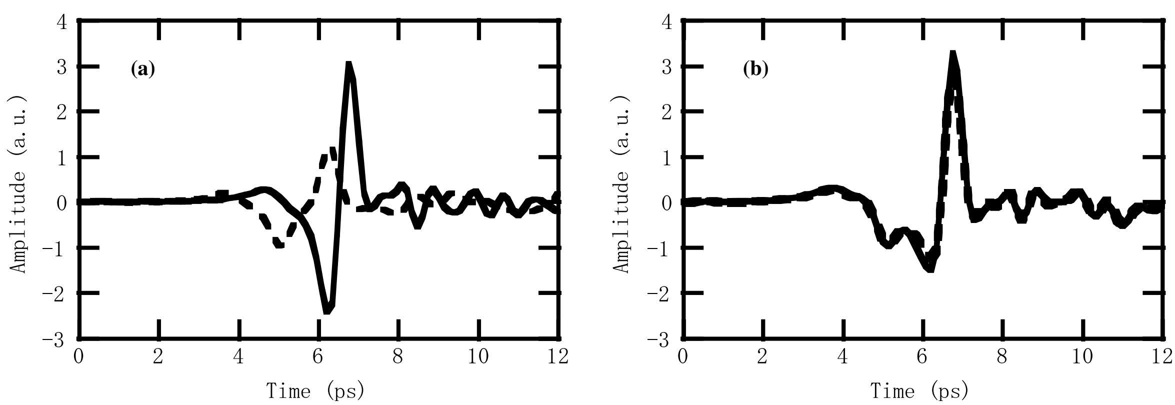

Fig. 6. (a) Temporal profiles of THz waves obtained using only one of the two sub-cross-sections. The solid curve is the THz waveform obtained using the outer part of the cross-section of the THz wave, and the dashed cure is that obtained using the inner part of the cross-section. (b) The temporal profile of the THz wave obtained without an aperture (solid curve), and that made by the summation of the two THz waves shown in (a) (dashed curve).

properties of the THz waves at all frequencies. A similar method has been proposed by Lee and Shu for the optical region [17].

Next, we numerically simulate the complex THz waves shown by the solid curves in Fig. 2, using the temporal profiles of the THz waves shown in Fig. 6(a) and the idea of Eq. (1). We used following assumptions to simplify the calculation:

1. The spectral profiles of the THz wave in any small section within the inner (or outer) section are the same. (We note here that this is actually an assumption to simplify the calculation. The radial distribution of the THz wave in the collimated beam depends on the THz frequency, and is not uniformly distributed.)
2. The absorption coefficient and the refractive index of the masks used are independent of the THz wave frequency.

The THz wave $E_{mask}(t)$ generated by using a mask is therefore given by the following equation:

$$\begin{aligned}E_{mask}(t) = {} & (1 - S_{min}/S_{win})E_{in}(t) + (1 - S_{mout}/S_{wout})E_{out}(t) \\ & + A[(S_{min}/S_{win})E_{in}(t - t_{dy}) \\ & + (S_{mout}/S_{wout})E_{out}(t - t_{dy})] \qquad (2)\end{aligned}$$

Here, the cross-section of the THz wave before passing through a mask is divided into two sub-sections of S_{wout} and S_{win}. $E_{out}(t)$ and $E_{in}(t)$ are THz waveforms that have passed through only the outside and inside sections and are shown by the solid and dashed curves in Fig. 6(a), respectively. These waves $E_{out}(t)$ and $E_{in}(t)$ are those not modified by a mask. S_{min} is the masked area of the inner cross-section S_{win} covered by a mask, and S_{mout} is the masked area of the outer cross-section S_{wout} covered by a mask. $S_{wout}-S_{mout}$ ($S_{win}-S_{min}$) is the outer (inner) cross-section that was not covered by a mask. Therefore, the cross-section of the THz wave after passing through a mask is divided into four sub-sections of S_{mout}, S_{min}, $S_{wout}-S_{mout}$, and $S_{win}-S_{min}$. The definitions of parameters S_{win}, S_{wout}, S_{min}, and S_{mout} are also shown schematically in Fig. 5. Parameter A is the ratio of the magnitude of the peak amplitudes of the THz wave obtained with and without a mask and t_{dy} is the delay time of the peak of the THz wave caused by the mask.

The delay time t_{dy} and the ratio of the peak-to-peak amplitudes of the THz waves A induced by the masks were obtained by measuring the change of the peak amplitude and the temporal position of the peak THz waves obtained with and without the mask. The parameters t_{dy} and A were 1 ps and 0.80 for the calendar plate and 4 ps and 0.57 for the ruler. The simulated THz waves corresponding to the solid curves in Figs. 2(a)–(d) are shown by dashed curves in Figs. 2(a)–(d).

In spite of the simple assumptions made above, the overall agreement between the experimental and the simulated curves in Figs. 2 is satisfactory. The disagreement between them is attributed to the effects of the assumptions. The overall agreement between the experiment and the simulation of the THz waves shows that our method can be used to design more general waveforms of THz waves.

We have shown that various temporal waveforms can be synthesized based on the simple spatio-temporal properties of the THz waves. Our simple model expressed by Eq. (2) shows that we can design THz waveforms using numerical simulation, if we know the temporal and cross-sectional profiles of the THz waves and the time delay and decrease of the amplitude of the THz wave caused by the mask. Since Eq. (2) is simple, it is not a hard task to calculate it inversely to obtain the properties of a mask required for a given THz waveform.

Flexible and controllable design of temporal waveforms of laser pulses is often needed for the coherent control of the states of materials or the control of chemical reactions [18,19]. When we apply THz waves to such applications, we will also need complicated temporal waveforms. Our simple method will enable flexible and controllable design and generation of complex temporal THz waveforms and will be useful for such purposes.

4. Summary

We have shown that by using masks in a simple way, we can easily design and synthesize various temporal THz waveforms. Our method does not require sophisticated optics, such as millimeter-wave gratings and small size apertures. Plastic plates were used as amplitude-and-phase masks for the demonstration. Our method will be useful for controlling the state of materials when THz waves are used as control pulses.

References

[1] A.S. Weiling, D.H. Auston, J. Opt. Soc. Am. B 13 (1996) 2783.
[2] Y. Liu, S.–G. Park, A.M. Weiner, Opt Lett. 21 (1996) 1762.
[3] F. Eickemeyer, R.A. Kaindl, M. Woerner, T. Elsaesser, A.M. Weiner, Opt. Lett. 25 (2000) 1472.
[4] J.D. Mckinney, D.E. Leaird, A.M. Weiner, Opt. Lett. 27 (2002) 1345.
[5] J.O. White, C. Ludwig, L. Kuhl, J. Opt. Soc. Am. B 12 (1995) 1687.
[6] T.M. Goyette, W. Guo, F.C. De Lucia, J.C. Swartz, H.O. Everitt, B.D. Guenther, E.R. Brown, Appl. Phys. Lett. 67 (1995) 3810.
[7] J. Bromage, S. Radic, G.P. Agrawal, C.R. Stround Jr., P.M. Fauchet, R. Sobolewski, J. Opt. Soc. Am. B 15 (1998) 1953.
[8] T. Hattori, R. Rungsawang, K. Ohta, K. Tukamoto, Jpn. J. Appl. Phys. Part 1 41 (2002) 5198.
[9] H. Harde, D. Grishkowski, J. Opt. Soc. Am. B 8 (1991) 1642.
[10] J. Zielbauer, M. Wegener, Appl. Phys. Lett. 68 (1996) 1223.
[11] P.I. Tamborenea, H. Metiua, J. Chem. Phys. 110 (1999) 9202.
[12] R. Ascazubi, C.C. Akin, T. Zaman, R. Kersting, G. Strasser, Appl. Phys. Lett. 81 (2002) 4344.
[13] R.G. Brewer, A.Z. Genack, Phys. Rev. Lett. 36 (1976) 959.
[14] R. Yano, Y. Hirayama, S. Miyashita, H. Sasabu, N. Uesugi, S. Uehara, Phys. Lett. A 289 (2001) 93.
[15] P.U. Jepsen, S.R. Keiding, Opt. Lett. 20 (1995) 807.
[16] W. Demtröder, Laser Spectroscopy, third ed., Springer, Berlin, 2003, p. 102.
[17] K.-S. Lee, C. Shu, Appl. Phys. Lett. 78 (2001) 1041.
[18] K. Komori, T. Sugaya, M. Watanabe, T. Hidaka, Jpn. J. Appl. Phys. Part 1 4B (2000) 2347.
[19] M. Shapiro, P. Bruner, J. Chem. Soc. Faraday Trans. 93 (1997) 1263.
[20] J. Ahn, A.V. Efimov, R.D. Averitt, A.J. Taylor, Opt. Exp. 11 (2003) 2486.
[21] Soeren Keiding Grischkowsky, Martin van Exter, Ch. Fattinger, J. Opt. Soc. Am. B7 (1990) 2006.